

Genetic Algorithm Application in Multi-Objective Optimization of Structural Parameters and PID Controller Parameters on Bus Driver Seat's Suspension System

Ngoc Dai Pham

Lecturer
Department of Automotive Engineering,
Faculty of Transportation Engineering, Ho
Chi Minh City University of Technology
(HCMUT) – Vietnam National University Ho
Chi Minh City, 268 Ly Thuong Kiet Street,
District 10, Ho Chi Minh City
Vietnam

The driver seat's suspension system is optimized through a 3DOF quarter-vehicle model. The optimization's objectives are simultaneously minimizing the driver's acceleration and displacement. The elastic element's stiffness k_d (N/m) and the damper's damping coefficient c_d (Ns/m) are optimized by the Pareto Method with the objective function $J(x)$ designed by the Weighted Square Sum method, and the min value of $J(x)$ is found with the genetic algorithm (GA). A PID controller is integrated into the system to improve the working efficiency, and GA optimizes the controller parameters K_p , K_i , K_d , and N . The optimization processes were carried out under the condition of transient road excitation according to the IRC 99-1988 standard. The results showed that compared to the passive seat with the structural parameters optimized, the active seat with a PID controller reduced 80 - 88% vertical displacement at the driver's mass of 65 (kg), 100 (kg), and 72 - 84% at 80 (kg).

Keywords: Pareto, PID controller, genetic algorithm, multi-objective optimization, 3DOF quarter model.

1. INTRODUCTION

Vibration isolation systems at the driver's seat position, with the function of reducing vibrations transmitted from the vehicle to the driver's body, have long been studied and applied [1-5]. The seat suspension system can be divided into passive, semi-active, and fully active forms [6]. Currently, in Vietnam, the passive seat suspension system is commonly used. This type of seat suspension system has a natural frequency in a small range of 1.5 - 4 (Hz) [6,7]. Therefore, when the seat suspension system is excited in a small frequency range, it will amplify the vibrations transmitted to the driver's body instead of reducing the vibrations [6,7].

On the contrary, the passive seat suspension system effectively isolates high-frequency vibrations above 5 Hz [6,7]. In fact, the vibration transmitted from the road surface to the vehicle floor has a frequency in the range of 0.5 - 50 (Hz) [8], so to conclude the working efficiency of the seat suspension system, it is necessary to go through experimental measurements for each specific working condition [9-11]. The current passive seat suspension system's technical parameters, such as the stiffness of the elastic element and the damping coefficient of the shock absorber, can be justified by changing the air pressure and the opening of the damper element's throttle hole [7, 12].

However, the passive seat suspension system can

only change the optimal parameters according to the working conditions by the driver's perception, which does not respond optimally to reality. Analytical models are set up to determine specific parameters for each operating case. Among them is the study of analyzing the seat suspension system model to find the optimal structural parameters for many simultaneous operating conditions [12]. Optimizing simultaneously the parameters of the cabin and driver's seat vibration isolator using the 4DOF model [13]. Optimizing multiple parameters of the 7DOF quarter vehicle model using a genetic algorithm for the system with Pareto-type constraints using step and random excitations [14]. Optimizing the driver's seat suspension model with a scissor-oriented mechanism and a 4DOF decomposed human model to achieve the optimal pelvis acceleration value under the condition of vibration transmission limits in the frequency domain [15]. Optimization of the vehicle seat suspension system using the Particle Swarm Algorithm with a split-type occupant model to reduce the vibration transmitted to the driver's pelvis [16]. In addition, the vibration of the driver sitting on the locomotive seat with the suspension system is modeled and simulated, thereby proposing a simpler evaluation model [17]. Development of a simple nonlinear seat suspension system model in the longitudinal direction for wheel loader drivers when working on gravel roads [18]. In addition to optimizing vibration isolation models, studies integrating the system vibration controller are deployed [19-22]. The study points out the disadvantage of the H_∞ controller when amplifying noise in the finite frequency region and deploying the Output Feedback Controller [19]. Research on the application of the control system for seats on ground vehicles

Received: November 2024, Accepted: June 2025

Correspondence to: Ngoc Dai Pham, Faculty of Transportation Engineering, University of Technology, 268 Ly Thuong Kiet Street, District 10, Ho Chi Minh City, Vietnam. E-mail: phamngocdai@hcmut.edu.vn

doi: 10.5937/fme2503426D

© Faculty of Mechanical Engineering, Belgrade. All rights reserved

FME Transactions (2025) 53, 426-436 426

subjected to vibration contributes to reducing the impact of vibration in the low-frequency region [20]. Research on the application of sliding mode control in reducing vibration transmitted from the vehicle floor to the human body with the decomposed human model [21]. Research on the application of a semi-active control system in controlling the electromagnetic damping state to reduce vibration of the seat suspension system on ground machines subjected to vibration [22]. Research on controller design based on Projective Chaos Synchronization to reduce the power spectrum of human body acceleration on a 1DOF model [23].

The optimization and control studies in the driver's seat suspension system mentioned above show great interest in providing an optimal feeling for the driver and protecting their health from vibration factors. However, currently, in Vietnam, the research on optimization and control of the seat suspension system for specific cases still needs to be improved. In addition, the above studies also show that the responses of the suspension system, such as the acceleration of the occupant, the displacement of the seat surface, and the relative displacement of the suspension system, do not reach the optimal values at the same time. They can only be prioritized depending on the operating situation. In addition, the process of developing and applying controllers to the suspension system encounters difficulties in the stage of determining the optimal parameters of the controllers. Therefore, this study has proposed a Pareto application method to simultaneously optimize multiple objectives of the suspension according to the required weighting factors. In addition, the study has proposed a method of applying the genetic algorithm (GA) to determine multiple technical parameters of the structure and the controller simultaneously. This study can be applied to the process of calculating and selecting structural parameters as well as the process of designing control systems applied to seat suspension systems in practice.

2. SIMULATION MODEL

2.1 3DOF quarter-vehicle model and controller

The simulation model of the bus driver seat's suspension system is integrated into the 2DOF quarter-vehicle model, becoming a 3DOF model [24], Figure 1. The seat suspension system and the driver are considered separately as a spring-mass-damper system to precisely evaluate the behavior of the driver and the seat's suspension system when vibrations are transmitted from the wheel to the vehicle body and transmitted to the driver's seat. The seat suspension system is optimized through the integration of a support system to control displacement and seat acceleration, including an actuator system simulated in the form of force F (N) and a PID controller (proportional-integral-derivative controller).

2.2 Mathematical model

The physical model of Figure 1 is converted into a mathematical model through the technical parameters of

the elements that make up the model, such as mass elements, stiffness elements, and damping elements.

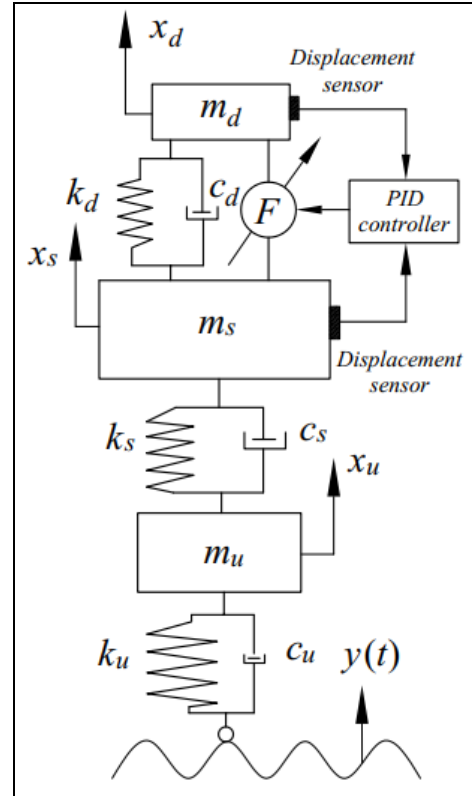


Figure 1. 3DOF quarter-vehicle model and PID controller [24]

Apply the general form of Lagrange's equation according to (1) to the system of Figure 1. f_r, \dot{q}_r, q_r are generalized force, generalized velocity, and generalized coordinate are, respectively.

$$\frac{d}{dt} \left(\frac{\partial K}{\partial \dot{q}_r} \right) - \frac{\partial K}{\partial q_r} + \frac{\partial D}{\partial \dot{q}_r} + \frac{\partial V}{\partial q_r} = f_r \quad (1)$$

The kinetic energy K , potential energy V , and dissipation function D of the mechanical system are respectively computed as follows.

$$K = \frac{1}{2} m_u \dot{x}_u^2 + \frac{1}{2} m_s \dot{x}_s^2 + \frac{1}{2} m_d \dot{x}_d^2 \quad (2)$$

$$V = \frac{1}{2} k_u (x_u - y)^2 + \frac{1}{2} k_s (x_s - x_u)^2 + \dots + \frac{1}{2} k_d (x_d - x_s)^2 \quad (3)$$

$$D = \frac{1}{2} c_u (\dot{x}_u - \dot{y})^2 + \frac{1}{2} c_s (\dot{x}_s - \dot{x}_u)^2 + \dots + \frac{1}{2} c_d (\dot{x}_d - \dot{x}_s)^2 \quad (4)$$

The first derivative of the kinetic energy function K with respect to the variable $\dot{x}_u, \dot{x}_s, \dot{x}_d$ (5).

$$\frac{\partial K}{\partial \dot{x}_u} = m_u \dot{x}_u; \frac{\partial K}{\partial \dot{x}_s} = m_s \dot{x}_s; \frac{\partial K}{\partial \dot{x}_d} = m_d \dot{x}_d \quad (5)$$

The first derivative of the kinetic energy function K with respect to the variable x_u, x_s, x_d (6).

$$\frac{\partial K}{\partial x_u} = 0; \frac{\partial K}{\partial x_s} = 0; \frac{\partial K}{\partial x_d} = 0 \quad (6)$$

The first derivative of the potential energy function V with respect to the variable x_u, x_s, x_d (7).

$$\begin{aligned} \frac{\partial V}{\partial x_u} &= k_u(x_u - y) - k_s(x_s - x_u) \\ &= (k_u + k_s)x_u - k_s x_s - k_u y \\ \frac{\partial V}{\partial x_s} &= k_s(x_s - x_u) - k_d(x_d - x_s) \\ &= -k_s x_u + (k_s + k_d)x_s - k_d x_d \\ \frac{\partial V}{\partial x_d} &= k_d(x_d - x_s) = -k_d x_s + k_d x_d \end{aligned} \quad (7)$$

The first derivative of the dissipation function D with respect to the variable $\dot{x}_u, \dot{x}_s, \dot{x}_d$ (8).

$$\begin{aligned} \frac{\partial D}{\partial \dot{x}_u} &= c_u(\dot{x}_u - \dot{y}) - c_s(\dot{x}_s - \dot{x}_u) \\ &= (c_u + c_s)\dot{x}_u - c_s \dot{x}_s - c_u \dot{y} \end{aligned}$$

$$\begin{aligned} \frac{\partial D}{\partial \dot{x}_s} &= c_s(\dot{x}_s - \dot{x}_u) - c_d(\dot{x}_d - \dot{x}_s) \\ &= -c_s \dot{x}_u + (c_s + c_d)\dot{x}_s - c_d \dot{x}_d \end{aligned} \quad (8)$$

$$\frac{\partial D}{\partial \dot{x}_d} = c_d(\dot{x}_d - \dot{x}_s) = -c_d \dot{x}_s + c_d \dot{x}_d$$

Road surface excitation $y(t)$ is applied according to the IRC 99 – 1988 standard [25] with a mathematical model according to (9). In which $d_1 = 0.5$ (m) – length of the bump, $d_2 = 0.05$ (m) – height of the bump, $v = 40$ (km/h) – vehicle's average velocity, t (s) – time.

$$y(t) = \begin{cases} d_2 \sin^2 \frac{\pi v}{d_1} t; & 0 \leq t < \frac{d_1}{v} \\ 0; & t < 0, t \geq \frac{d_1}{v} \end{cases} \quad (9)$$

The dynamic equation of motion of the mechanical system when subjected to road surface excitation is written in general form according to (10). At the same time, model (10) is converted to a state-space model for control according to (11).

$$M\ddot{X} + C\dot{X} + KX = U$$

$$\begin{bmatrix} m_u & 0 & 0 \\ 0 & m_s & 0 \\ 0 & 0 & m_d \end{bmatrix} \begin{bmatrix} \ddot{x}_u \\ \ddot{x}_s \\ \ddot{x}_d \end{bmatrix} + \begin{bmatrix} c_u + c_s & -c_s & 0 \\ -c_s & c_s + c_d & -c_d \\ 0 & -c_d & c_d \end{bmatrix} \begin{bmatrix} \dot{x}_u \\ \dot{x}_s \\ \dot{x}_d \end{bmatrix} + \begin{bmatrix} k_u + k_s & -k_s & 0 \\ -k_s & k_s + k_d & -k_d \\ 0 & -k_d & k_d \end{bmatrix} \begin{bmatrix} x_u \\ x_s \\ x_d \end{bmatrix} = \begin{bmatrix} c_u \dot{y} + k_u y \\ F \\ -F \end{bmatrix} \quad (10)$$

$$\dot{X} = A.X + B.F + D.d$$

$$\begin{bmatrix} \dot{x}_u \\ \ddot{x}_u \\ \dot{x}_s \\ \ddot{x}_s \\ \dot{x}_d \\ \ddot{x}_d \end{bmatrix} = \begin{bmatrix} 0 & 1 & 0 & 0 & 0 & 0 \\ \frac{-k_u - k_s}{m_u} & \frac{-c_u - c_s}{m_u} & \frac{k_s}{m_u} & \frac{c_s}{m_u} & 0 & 0 \\ 0 & 0 & 0 & 1 & 0 & 0 \\ \frac{k_s}{m_s} & \frac{c_s}{m_s} & \frac{-k_s - k_d}{m_s} & \frac{-c_s - c_d}{m_s} & \frac{k_d}{m_s} & \frac{c_d}{m_s} \\ 0 & 0 & 0 & 0 & 0 & 1 \\ 0 & 0 & \frac{k_d}{m_d} & \frac{c_d}{m_d} & \frac{-k_d}{m_d} & \frac{-c_d}{m_d} \end{bmatrix} \begin{bmatrix} x_u \\ \dot{x}_u \\ x_s \\ \dot{x}_s \\ x_d \\ \dot{x}_d \end{bmatrix} + \begin{bmatrix} 0 \\ 0 \\ 0 \\ 1 \\ 0 \\ -1 \end{bmatrix} F + \begin{bmatrix} 0 \\ 1 \\ 0 \\ 0 \\ 0 \\ 0 \end{bmatrix} (c_u \dot{y} + k_u y) \quad (11)$$

3. PARAMETERS OPTIMIZATION

3.1 Pareto optimization

The study optimizes the technical parameters of the seat suspension system, k_d , and c_d . The goal of the optimization process is to simultaneously minimize the seat acceleration value \ddot{x}_d (m/s²) - $\mu_1(x)$ and the seat displacement x_d (m) - $\mu_2(x)$ with the constraint condition ensuring the stability of the human body on the seat surface $\ddot{x}_d / g \leq 1$. The relationship between the structural parameters (k_d, c_d), the optimization objective ($\mu_1(x), \mu_2(x)$), and the constraint condition $\ddot{x}_d / g \leq 1$ is shown in (12), (13), (14).

$$\begin{aligned} \text{Min}_x [\mu_1(x) \quad \mu_2(x) \quad \dots \quad \mu_n(x)], n = 2 \\ \mu_1(x) = \text{Max}(\ddot{x}_d), \mu_2(x) = \text{Max}(x_d) \end{aligned} \quad (12)$$

$$x = [x_1 \quad x_2] = [k_d \quad c_d] \quad (13)$$

$$\ddot{x}_d / g \leq 1 \quad (14)$$

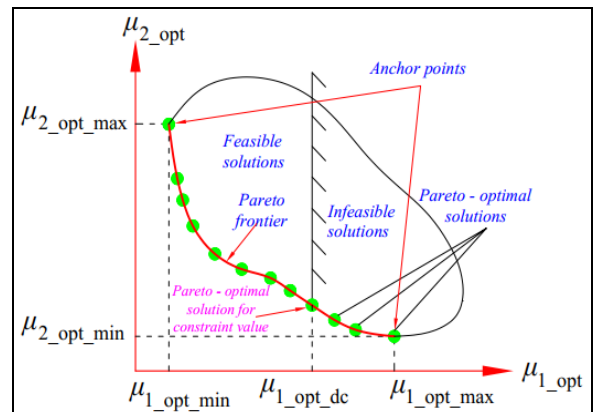


Figure 2. Pareto optimal solutions [26]

The relationship between $\mu_1(x)$ and $\mu_2(x)$ in the system of Figure 1 is explained in Figure 2. When the optimal value of the target $\mu_1(x)$ reaches the smallest value, the optimal value of the target $\mu_2(x)$ reaches the most significant value, x_{dmax} , and vice versa. Thus, these two targets cannot simultaneously achieve the smallest values with the same set of structural parameters k_d, c_d . The study applies the Pareto multi-objective optimization method to solve this problem. The selected optimization model has the form of a Weighted Square Sum according to [26], and the new optimization objective is used according to (15). However, the maximum acceleration value and the seat displacement are not in the same unit of measurement, so the magnitude of change is different, and they cannot be used for direct evaluation when entering the model (15). Therefore, the study linearizes the optimization model with coefficients u_1 and u_2 according to (16) and (17) [26]. In this optimization problem, the value of the weighting factor w affects the priority level of each objective; the larger the priority level, the smaller the value of the optimal objective achieved, and vice versa.

$$\text{Min}_x J(x) = wu_1^k [\mu_1(x)] + (1-w)u_2^k [\mu_2(x)] \quad (15)$$

$$u_1 [\mu_1(x)] = \frac{[\text{Max}(\ddot{x}_d)]_{\text{max}} - \text{Max}(\ddot{x}_d)}{[\text{Max}(\ddot{x}_d)]_{\text{max}} - [\text{Max}(\ddot{x}_d)]_{\text{min}}} \quad (16)$$

$$u_2 [\mu_2(x)] = \frac{(\text{Max}|x_d|)_{\text{max}} - \text{Max}|x_d|}{(\text{Max}|x_d|)_{\text{max}} - (\text{Max}|x_d|)_{\text{min}}} \quad (17)$$

3.2 PID controller design

The proportional-integral-derivative controller consists of three separate parts: proportional part P , integral part I , and derivative part D [27]. With the error value [$e(t) = x_d$ (m)] of the output signal x_d (m) compared to the set value 0 (m), the combined effect of the three values P , I , and D is used as the control signal for the seat suspension system in the form of force $F(N)$, according to (18).

$$F(t) = K_P e(t) + K_I \int_0^t e(t) dt + N K_D (e(t) - N e^{-Nt}) \quad (18)$$

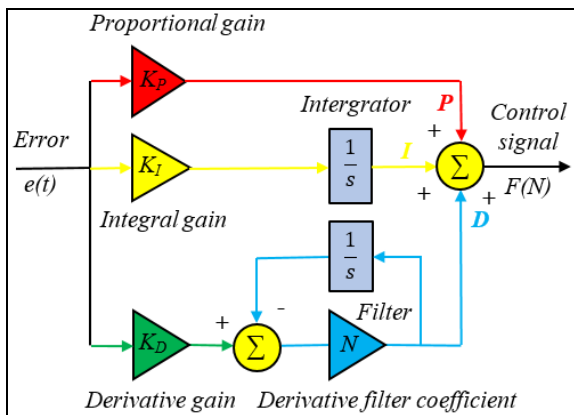


Figure 3. The structure of the PID controller [27]

Performing the Laplace transform of equation (18) obtains the transfer function of the control force $F(t)$ and the error value $e(t)$ according to (19).

$$TF = \frac{F(s)}{e(s)} = \left[K_P + K_I \left(\frac{1}{s} \right) + K_D \left(\frac{Ns}{s+N} \right) \right] \quad (19)$$

The mathematical model according to (18) and the transfer function model according to (19) are applied using Matlab Simulink as Figure 3.

3.3 Genetic algorithm and optimization standards

In evaluating the performance of the PID controller during operation, criteria such as Integral Absolute Error (IAE), Integral Square Error (ISE), Integral Time Absolute Error ($ITAE$), and Integral Time Square Error ($ITSE$) are commonly used [28]. Within the scope of the study, the $ITAE$ criterion is chosen to find the optimal parameters K_P, K_I, K_D , and N in the investigated domain using the genetic algorithm GA . The criteria $ITAE$ are calculated according to (20).

$$J_{ITAE} = \int_0^{+\infty} t|e(t)|dt \quad (20)$$

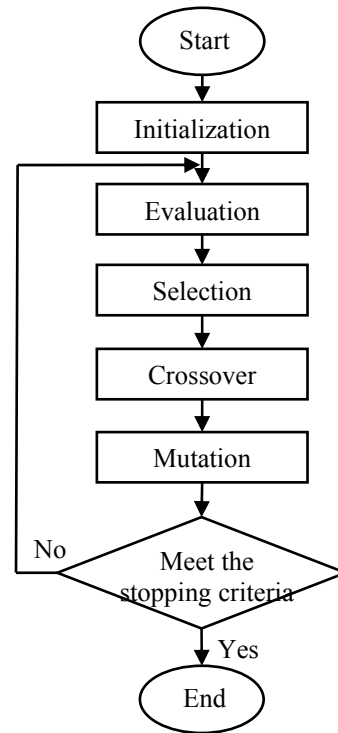


Figure 4. Genetic algorithm diagram [27]

Table 1. GA's parameters

Option	Value/ type			
	Structure optimal	PID	PI	PD
No of variables	2	4	2	2
Population size	10	15	15	15
Generation size	15	20	20	20
Crossover	0.8	0.8	0.8	0.8
Mutation	0.1	0.1	0.1	0.1
Fitness function	J_x	J_{ITAE}	J_{ITAE}	J_{ITAE}

Genetic algorithm, Figure 4, serves to find appropriate solutions to combinatorial optimization problems by applying evolutionary principles such as Heredity, Mutation, Selection, and Crossover [26, 28]. Accor-

dingly, the suitability of GA in the problem of finding multiple optimal parameters, such as k_d and c_d for an overall objective such as $J(x)$ and K_p, K_I, K_D , and N , with the $ITAE$ objective, is analyzed. The algorithm's parameters, as well as the searched limits for system structure and controller parameters, are summarized in Tables 1 and 2.

Table 2. Parameter's search region with GA

	Lower bound	Upper bound
k_d	24000 (N/m)	63000 (N/m)
c_d	300 (Ns/m)	2000 (Ns/m)
K_p	0	200000
K_I	0	1200000
K_D	0	8000
N	0	1000

4. RESULTS AND DISCUSSIONS

4.1 System optimization with GA

Choose a typical case with $w = 1$ for equation (14) and perform the search for the optimal J_{opt} value with the GA genetic algorithm. The convergence of the search results is shown in Figure 5. Accordingly, for each value of w , the optimal J_{opt} is obtained simultaneously with the parameter set k_{d_opt}, c_{d_opt} , and μ_{1_opt}, μ_{2_opt} . In the case of optimizing the structural parameters when choosing the initial Population value of 10, the GA algorithm gives the search results that start to converge at the tenth generation for all 03 cases of driver mass. Summing all cases of w in the region $w \in [0 \div 1]$, Figure 6 is obtained. Figure 6 shows the relationship between the optimal cases of acceleration μ_{1_opt} and seat displacement μ_{2_opt} with the driver mass of 65 (kg), 80 (kg), and 100 (kg) across the entire survey domain of k_d and c_d . Accordingly, in all 03 cases of driver mass, the trends of μ_{1_opt} and μ_{2_opt} are always opposite and do not simultaneously reach the same minimum state with the same w .

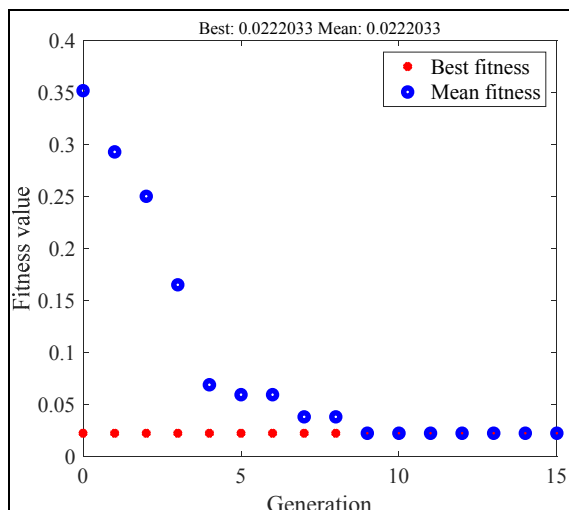


Figure 5. The convergence of value J_{opt} with GA

The results in Figure 8 show that when $w = 1$ - prioritizing acceleration optimization, the maximum acceleration response value over time at all investigated masses is the smallest, and the maximum displacement

is the largest. This result is similar to $w = 0$, prioritizing seat displacement optimization.

The optimal values for the cases of w corresponding to $m_d = [65, 80, 100]$ (kg) are summarized in Table 3.

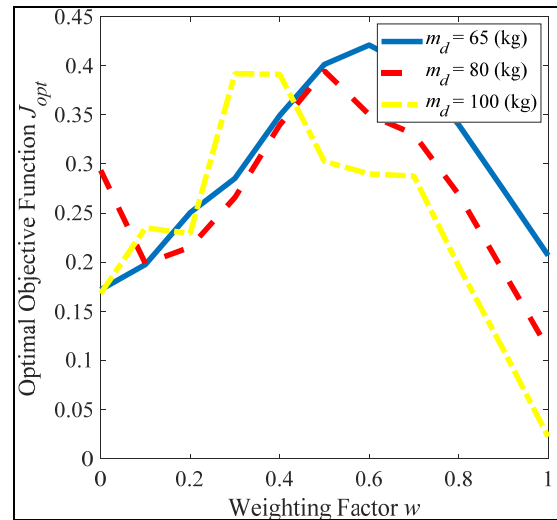


Figure 7. The change of J_{opt} according to w

The increase of the w value leads to a greater priority for the seat acceleration target μ_1 and vice versa. Thus, according to Figure 7, the greater the priority for acceleration with the value $w \in [0 \div 0.6]$, the larger the overall target value J_{opt} is, and gradually decreases in the region $w \in [0.6 \div 1]$, reaching a minimum at $w = 1$. The study chooses the case of value $w = 0.5$ to obtain the optimal k_{d_opt} and c_{d_opt} data for the next steps. With the optimal results obtained in the optimal cases of w , the acceleration and displacement values over time are shown in Figure 8.

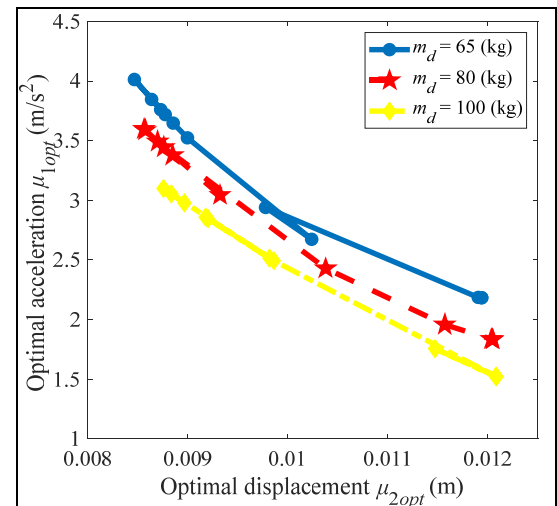


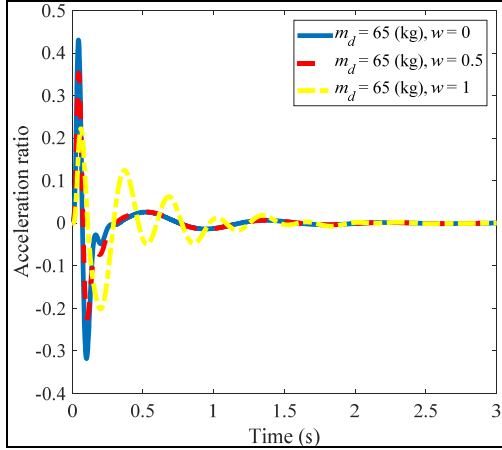
Figure 6. Pareto frontier

Table 3. Summary table of optimal values with GA

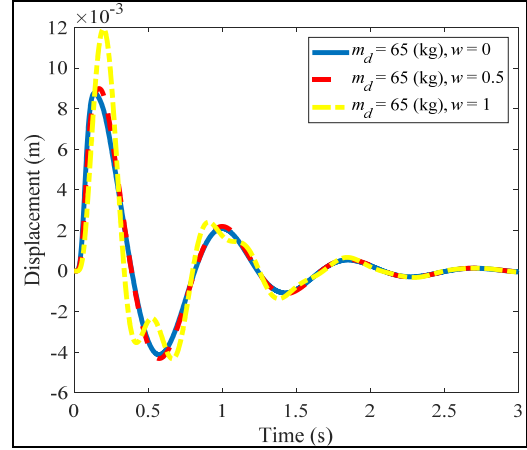
m_d (kg)	w	J_{opt}	k_{d_opt} (N/m)	c_{d_opt} (Ns/m)	μ_{1_opt} (m)	μ_{2_opt} (m/s ²)
65	0	0.1719	38878	1910	4.22	0.0088
80		0.2936	33277	1460	3.25	0.0093
100		0.1681	27228	2000	3.09	0.0088
65	0.1	0.1977	29254	1771	3.89	0.0086
80		0.1984	28212	1883	3.50	0.0087
100		0.2349	26946	1772	2.90	0.0090
65	0.2	0.2505	24000	1552	3.55	0.0087
80		0.2153	24000	1888	3.41	0.0086

100		0.2293	24000	1791	2.86	0.0088
65		0.2854	26344	1868	3.91	0.0085
80	0.3	0.2659	25825	1962	3.51	0.0086
100		0.3920	35463	1318	2.72	0.0098
65		0.3494	24930	1474	3.50	0.0089
80	0.4	0.3396	29296	1762	3.42	0.0088
100		0.3919	46685	1998	3.46	0.0092
65		0.4014	26608	1406	3.47	0.009
80	0.5	0.3948	32057	1916	3.60	0.0088
100		0.3026	25056	1521	2.65	0.0092
65		0.4210	26117	765	2.74	0.0102
80	0.6	0.3502	24000	753	2.66	0.0104
100		0.2899	24000	1044	2.18	0.0099

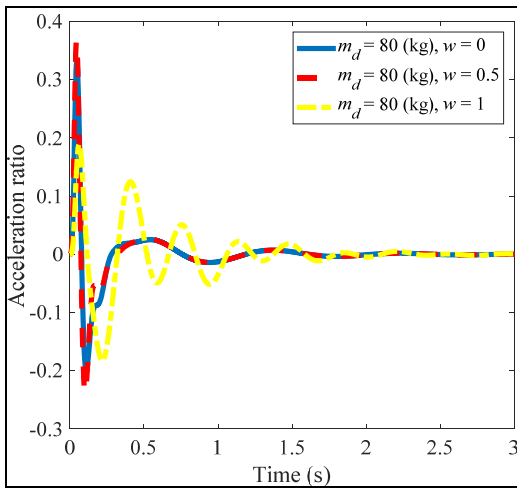
65		0.3972	24000	917	2.84	0.0098
80	0.7	0.3303	24000	405	1.92	0.0116
100		0.2878	24000	301	1.55	0.0121
65		0.3399	24000	307	2.19	0.0119
80	0.8	0.2690	24000	302	1.86	0.0120
100		0.1960	24213	451	1.65	0.0115
65		0.2736	24000	300	2.18	0.0119
80	0.9	0.1904	24000	300	1.85	0.0120
100		0.1108	24000	300	1.55	0.0121
65		0.2068	24000	300	2.18	0.0119
80	1	0.1116	24000	300	1.85	0.0120
100		0.0222	24000	300	1.55	0.0121



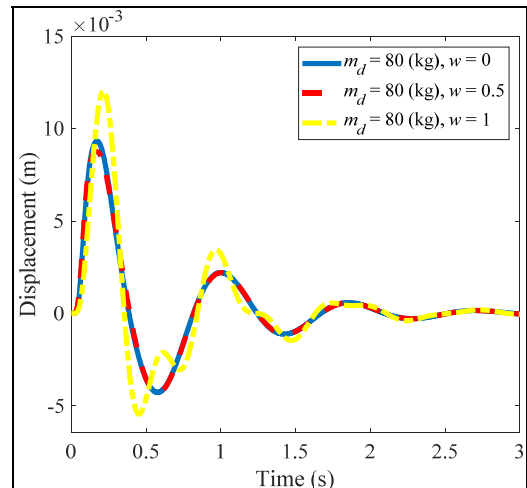
a) Acceleration ratio, $m_d = 65$ (kg)



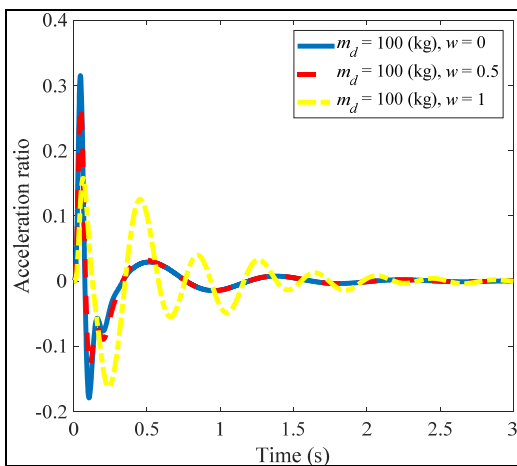
b) Displacement, $m_d = 65$ (kg)



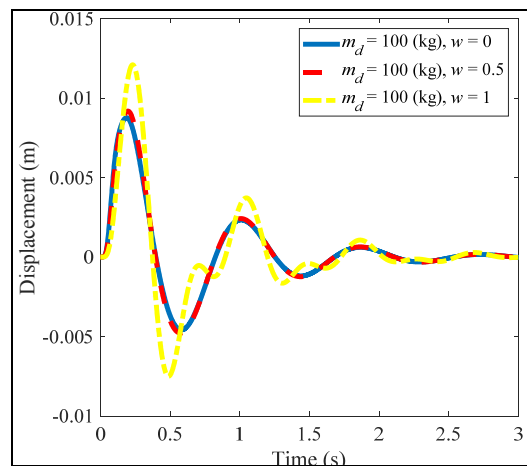
c) Acceleration ratio, $m_d = 80$ (kg)



d) Displacement, $m_d = 80$ (kg)



e) Acceleration ratio, $m_d = 100$ (kg)



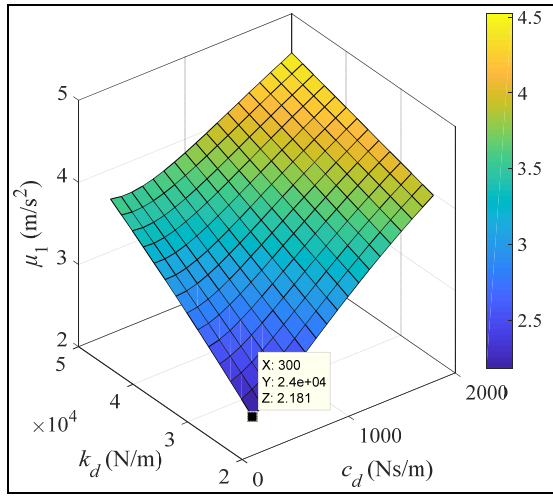
f) Displacement, $m_d = 100$ (kg)

Figure 8. Acceleration ratio and displacement over time with k_{d_opt} c_{d_opt} $w = [0 \ 0.5 \ 1]$, $m_d = [65 \ 80 \ 100]$ (kg)

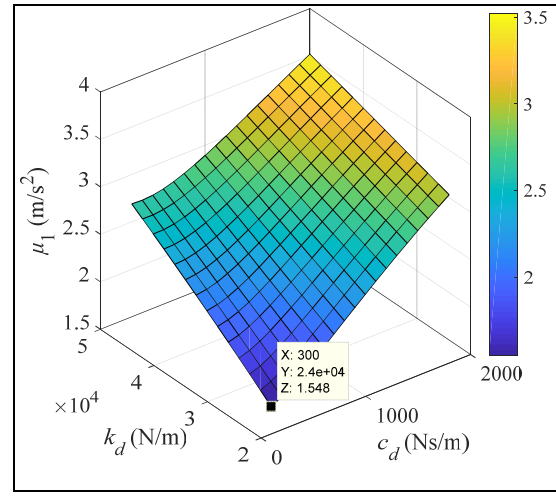
4.2 Comparing results between GA and the conventional method

With the input parameters of the GA algorithm according to Table 1, the optimal parameter results obtained according to Table 3 are compared with the conventional survey

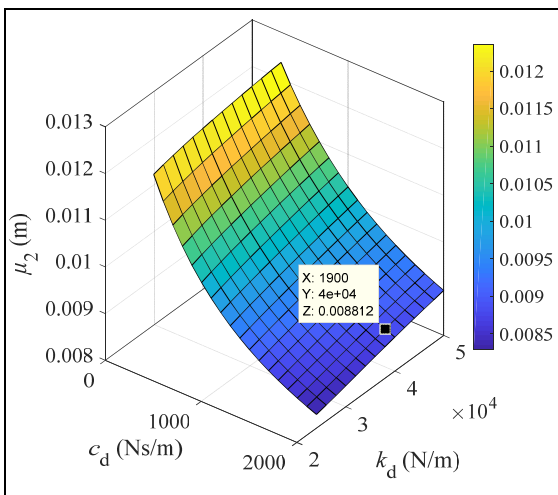
method on the entire range of k_d and c_d values. Accordingly, the survey points performed at $w = [0 \ 1]$, Figure 9, give the results of μ_{1_opt} close to the results according to GA in Table 3. However, with the same conditions, the values of μ_{2_opt} and J_{opt} are in the smallest region.



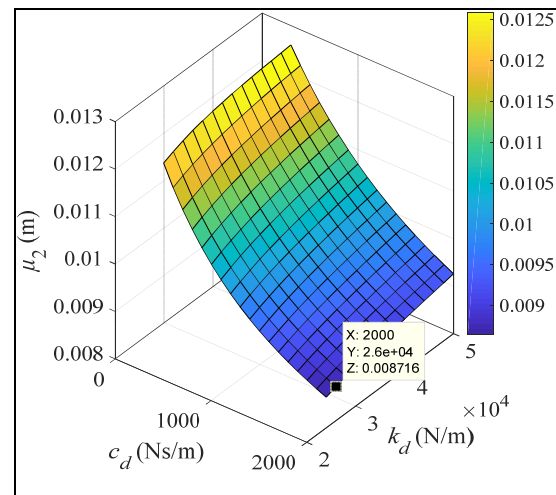
a) $w = 1, m_d = 65$ (kg)



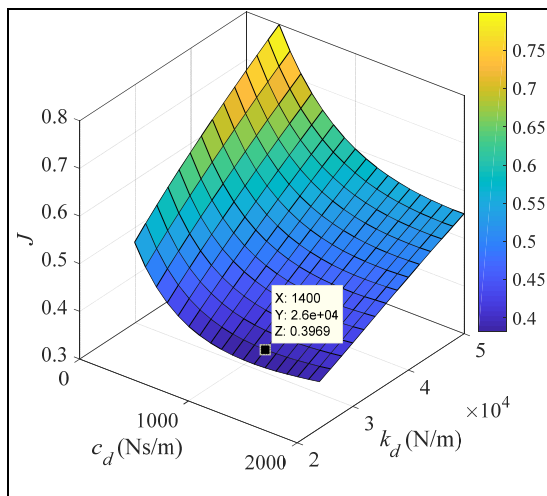
b) $w = 1, m_d = 100$ (kg)



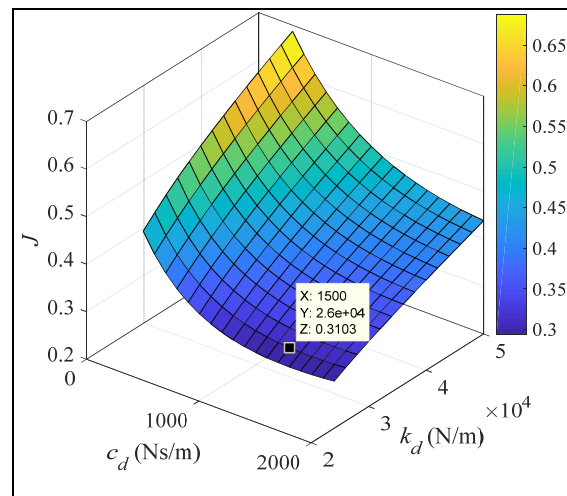
c) $w = 0, m_d = 65$ (kg)



d) $w = 0, m_d = 100$ (kg)



e) $w = [0 \ 1], m_d = 65$ (kg)



f) $w = [0 \ 1], m_d = 100$ (kg)

Figure 9. Comparing the results of the conventional survey method with GA, $m_d = 65$ (kg), 100 (kg)

4.3 PID, PI, PD controllers optimization with GA

The results of optimizing the coefficients of each controller with *GA* are summarized in Table 4.

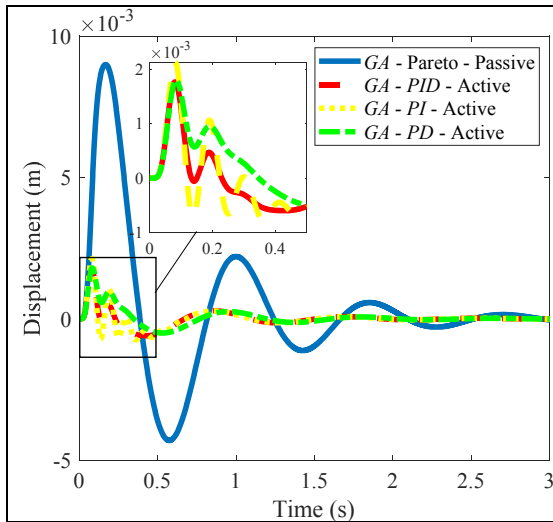
Table 4. Controller optimization results summary

$m_d = 65$ (kg)			
	<i>GA-PID</i>	<i>GA-PI</i>	<i>GA-PD</i>
K_P	188962	192323	190044
K_I	1147366	1076411	--
K_D	1467	--	1789
N	311	--	--
J_{ITAE}	0.000284	0.000289	0.000293
$m_d = 80$ (kg)			
	<i>GA-PID</i>	<i>GA-PI</i>	<i>GA-PD</i>
K_P	178281	180884	193785
K_I	1033332	1164391	--
K_D	781	--	744
N	339	--	--
J_{ITAE}	0.000304	0.000299	0.000285
$m_d = 100$ (kg)			
	<i>GA-PID</i>	<i>GA-PI</i>	<i>GA-PD</i>
K_P	197227	176872	190116
K_I	1077710	1074603	--

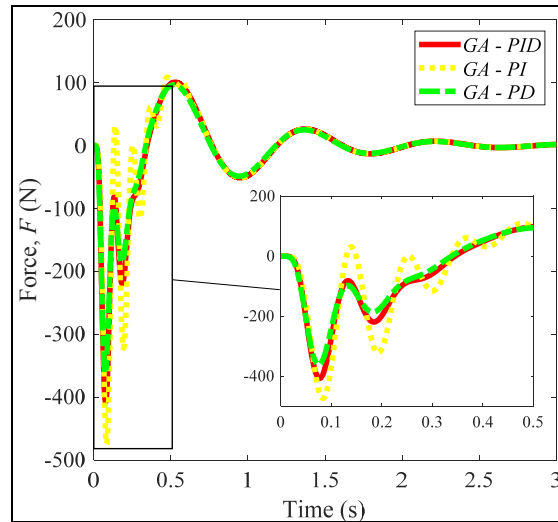
K_D	1367	--	7694
N	903	--	--
J_{ITAE}	0.000280	0.000309	0.000291

The influence of the controller on the displacement behavior of the seat surface, as well as the control signal value F (N), is shown in the case of $m_d = [65\ 80\ 100]$ (kg), $w = 0.5$ in Figure 10.

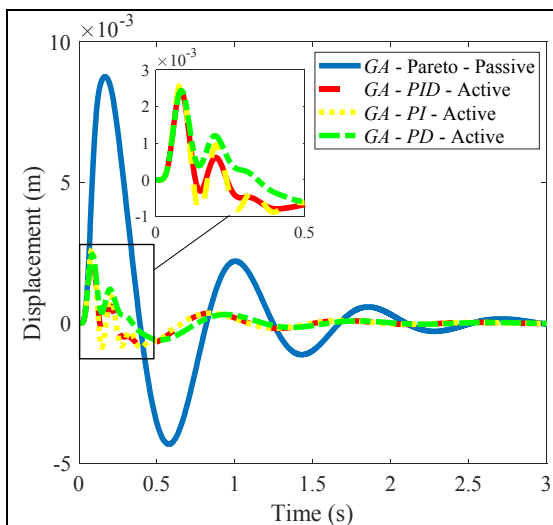
Figure 10 shows that, with the controllers, the maximum displacement of the seat surface is significantly reduced, thereby making the driver more stable and creating a better driving feeling. In detail, when comparing the 03 controllers, it can be seen that in the time range from 0 - 0.5 (s), the *PI* controller produces the worst response with the largest maximum vibration amplitude and the lowest stability. The *PD* controller has a lower maximum vibration amplitude than the *PID*, but the amplitude reduction time is slower than the *PID*. The control signal value F (N) of the three cases of the highest mass magnitude is below 600 (N). In which the *PD* controller needs the lowest force value and increases gradually according to the *PID* and *PI* controllers.



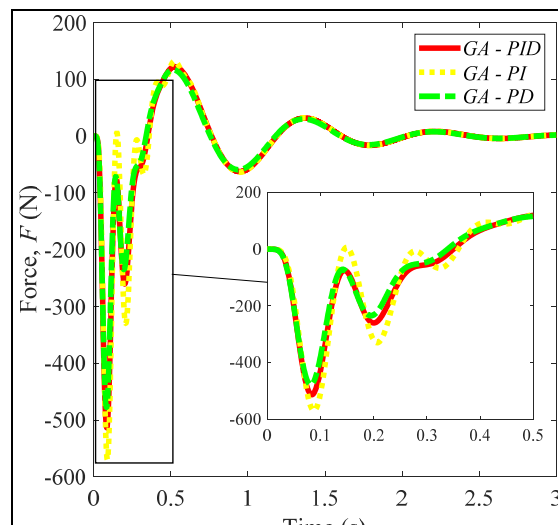
a) Displacement (m), $m_d = 65$ (kg)



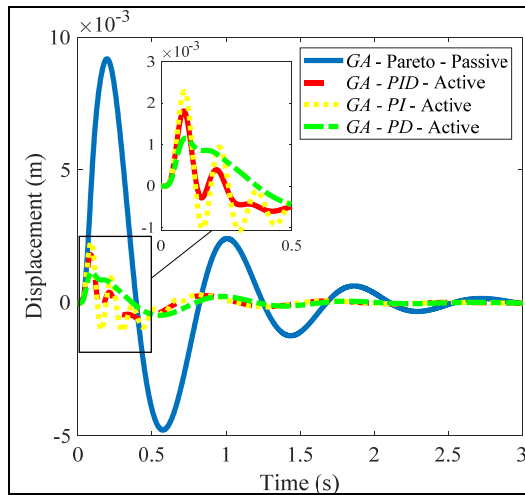
b) Control signal F (N), $m_d = 65$ (kg)



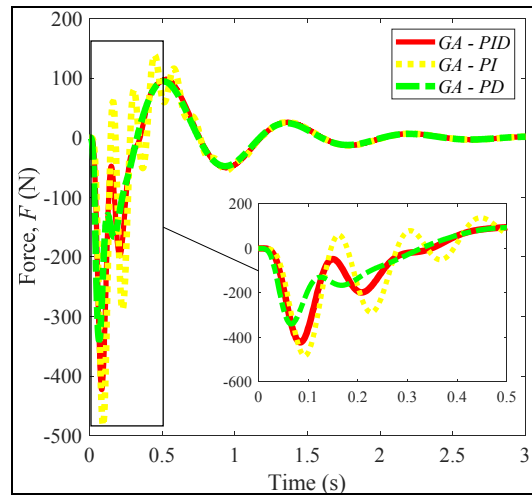
c) Displacement (m), $m_d = 80$ (kg)



d) Control signal F (N), $m_d = 80$ (kg)



e) Displacement (m), $m_d = 100$ (kg)

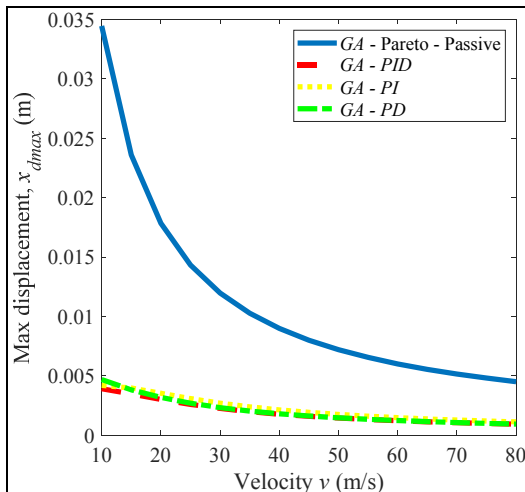


f) Control signal F (N), $m_d = 100$ (kg)

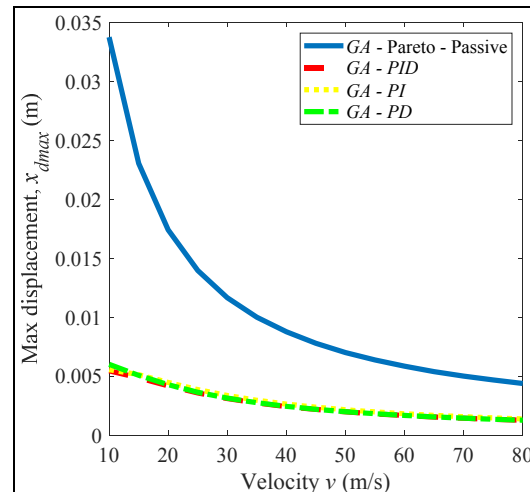
Figure 10. Seat displacement response over time with GA – PID, GA – PI, GA – PD controller

Based on the values of K_p , K_I , K_D , N , and $c_{d,opt}$, $k_{d,opt}$ just found, the survey of the seat displacement response over the entire vehicle speed range $v \in (10;80)$ (km/h) was conducted, and the results were shown in Figure 11. The results in Figure 11 show that, in all 03 cases of the surveyed driver mass $m_d = [65 \ 80 \ 100]$ (kg), with the

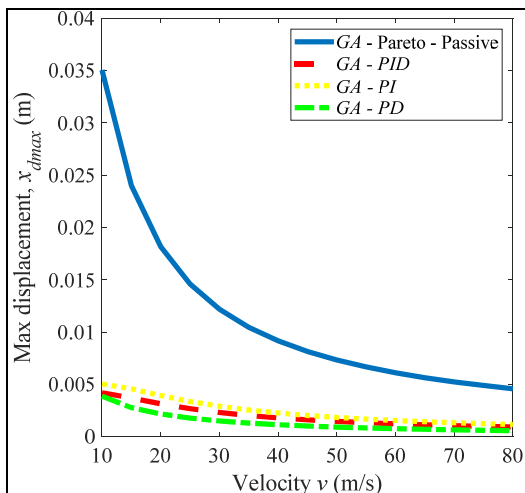
integrated controller, the maximum seat displacement is always smaller than that of the passive seat suspension system over the entire vehicle speed range. The amplitude reduction is in the range of 80% - 88% for the driver mass of 65 (kg), 100 (kg), and 72% - 84% for the driver mass of 80 (kg).



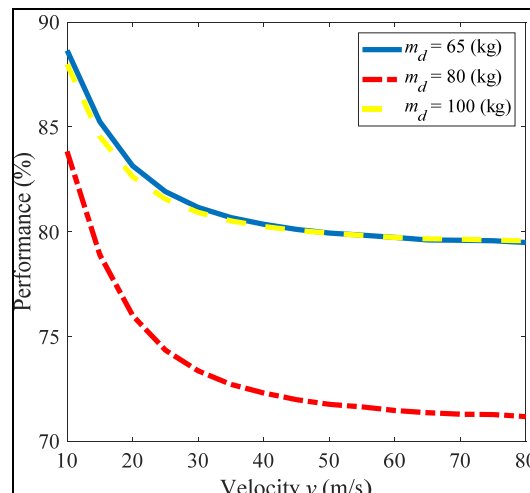
a) $m_d = 65$ (kg)



b) $m_d = 80$ (kg)



c) $m_d = 100$ (kg)



d) Performance of active systems (%)

Figure 11. Seat displacement response over the speed domain and the efficiency of GA – PID, GA – PI, GA – PD controllers

5. CONCLUSIONS

The study applied the genetic algorithm *GA* to optimize the technical parameters k_d , c_d of the seat's suspension system on the 3DOF model according to two objectives: reducing acceleration and seat displacement when subjected to transient excitation. At the same time, with the optimal structural parameter set k_{d_opt} , c_{d_opt} , the study integrated the *PID*, *PI*, and *PD* controllers to improve the reduction of seat displacement amplitude with the optimal parameters K_p , K_i , K_D , and N also searched by *GA*. The optimization results show that:

* Structural parameter optimization: The minimum optimal displacement and acceleration values of the seat surface μ_{1_opt} and μ_{2_opt} are not simultaneously achieved with the same pair of k_{d_opt} and c_{d_opt} values but vary in opposite directions. Therefore, the study applies the Pareto optimal multi-objective optimization model with the combined objective value $J(x)$ calculated by the Weighted Square Sum method in the weight domain $w \in [0;1]$. Depending on the use case, the selected w value will determine the corresponding k_{d_opt} , c_{d_opt} , μ_{1_opt} , and μ_{2_opt} values.

* *PID* controller parameter optimization: *PID* controller parameters, including K_p , K_i , K_D , and N , are found by *GA* according to the *ITAE* standard with the J_{ITAE} objective function. Applying a *PID* controller to the seat suspension system helps significantly improve seat displacement behavior. Specifically, the amplitude reduction is 80% - 88% for driver mass $m_d = 65$ (kg), $m_d = 100$ (kg), and 72% - 84% for $m_d = 80$ (kg).

ACKNOWLEDGEMENT

We acknowledge Ho Chi Minh City University of Technology (HCMUT), VNU-HCM, for supporting this study.

REFERENCES

- [1] Taro, S., Yasuo, O., Hiroyuki, S.: Active Suspension of Truck Seat, *Transactions of The Japan Society of Mechanical Engineers Series C*, Vol. 62, No. 600, pp. 3132-3138, 1996.
- [2] Gunston, T., Rebelle, J., Griffin, M.: A comparison of two methods of simulating seat suspension dynamic performance, *Journal of Sound and Vibration*, Vol. 278, No. 1-2, 2004.
- [3] Ngoc Dai Pham, A comparison of vibration behavior of linear and nonlinear bus driver seat suspension system using the 5dof model, *FME Transactions*, Vol. 53, No. 2, pp. 196-211, 2025.
- [4] Ilic, Z., et al.: The efficiency of passive vibration damping on the pilot seat of piston propeller aircraft, *Measurement*, Vol. 95, pp. 21-32, 2017.
- [5] Ilic, Z., et al.: Potential connections of cockpit floor-seat on passive vibration reduction at a piston-propelled airplane, *Technical Gazette*, Vol. 21, No. 3, pp. 471-478, 2014.
- [6] Alireza, H., Xu, Q.: Review on Seat Suspension System Technology Development, *Applied Sciences*, Vol. 9, 2019.
- [7] Maciejewski, I., Meyer, L., Krzyzynski, T.: Modelling and multi-criteria optimisation of passive seat suspension vibro-isolating properties, *Journal of Sound and Vibration*, Vol. 324, No. 3-5, 2009.
- [8] Dragan, S., Vlastimir, D.: The Effect of Stiffness and Damping of the Suspension System Elements on the Optimisation of the Vibrational Behaviour of a Bus, *International Journal for Traffic and Transport Engineering*, Vol. 1, No. 4, pp. 231-244, 2011.
- [9] Olanrewaju O., Steven J., Marianne, M., Malcolm, P.: City bus driving and low back pain: A study of the exposures to posture demands, manual materials handling and whole-body vibration, *Applied Ergonomics*, Vol. 38, pp. 29-38, 2007.
- [10] Paddan, G., Griffin, M.: Evaluation of Whole-body vibration in vehicles, *Journal of Sound and Vibration*, Vol. 253, pp. 195-213, 2002.
- [11] Ornwipa, T., Ryan P., Randal P., Linda, B., Peter W.: Whole body vibration exposures in bus drivers: A comparison between a high-floor coach and a low-floor city bus, *International Journal of Industrial Ergonomics*, Vol. 43, pp. 9-17, 2013.
- [12] Igor, M., Tomasz, K: Application of the Pareto-optimal approach for selecting dynamic characteristics of seat suspension systems, *Vehicle System Dynamics: International Journal of Vehicle Mechanics and Mobility*, Vol. 49, pp. 1929-1950, 2011.
- [13] Zhao, L., Zhou, C., Yu, Y.: Damping Collaborative Optimization of Five-suspensions for Driver-seat-cab Coupled System, *Chinese Journal of Mechanical Engineering*, Vol. 29, No. 4, pp. 773-780, 2016.
- [14] Nagarkar, P., Patil, G., Zaware, P., Rahul, N.: Optimization of Non-linear Quarter Car Suspension – Seat – Driver Model, *Journal of Advanced Research*, Vol. 7, pp. 991-1007, 2016.
- [15] Hill, K., Dhingra, A.: Modeling, analysis and optimization of a scissors linkage seat suspension, *Engineering Optimization*, Vol. 35, No. 4, pp. 341-357, 2003.
- [16] Gohari, M., Rahman, R., Tahmasebi, M.: Off-Road Seat Suspension Optimization by Particle Swarm Algorithm, *Applied Mechanics and Materials*, Vol. 315, pp. 507-511, 2013.
- [17] Stein, G., Peter, M., Gunston, T., Badura, S.: Modelling and simulation of locomotive driver's seat vertical suspension vibration isolation system, *International Journal of Industrial Ergonomics*, Vol. 38, No. 5-6, pp. 384-395, 2008.
- [18] Stein, G., Peter, M.: Study of simultaneous shock and vibration control by a fore-and-aft suspension system of a driver's seat, *International Journal of Industrial Ergonomics*, Vol. 41, No. 5, pp. 520-529, 2011.
- [19] Weichao, S., Jinfu, L., Ye, Z., Huijun, G.: Vibration control for active seat suspension systems via dynamic output feedback with limited

frequency characteristic, *Mechatronics*, Vol. 21, No. 1, pp. 250-260, 2011.

- [20] Igor, M.: Active control of working machines seat suspension aimed at health protection against vibration, *PAMM*, Vol. 7, No. 1, pp. 4130017-4130018, 2007.
- [21] Seung-Bok, C., Young-Min, H.: Vibration control of electrorheological seat suspension with human-body model using sliding mode control, *Journal of Sound and Vibration*, Vol. 303, No. 1-2, pp. 391-404, 2007.
- [22] Mcmanus, S., Clair, K., Boileau, P., Boutin, J., Rakheja, S.: Evaluation of Vibration and Shock Attenuation Performance of A Suspension Seat With A Semi-Active Magnetorheological Fluid Damper, *Journal of Sound and Vibration*, Vol. 253, No. 1, pp. 313-327, 2002.
- [23] Wen, G., Yao, S., Zhang, Z., Yin, H., Chen, Z., Xu, H., Ma, C.: Vibration control for active seat suspension system based on projective chaos synchronisation, *International Journal of Vehicle Design*, Vol. 58, No. 1, pp. 1-14, 2012.
- [24] Reza, J.: *Vehicle Dynamics: Theory and Applications*, Springer, NY, 2008.
- [25] The Indian Roads Congress, IRC-99-1988, Tentative Guidelines on the Provision of Speed Breakers for Control of Vehicular Speeds on Minor Roads.
- [26] Achille, M.: *Optimization In Practice With MATLAB for Engineering Students And Professionals*, Cambridge University Press, USA, 2015.
- [27] Rabindra, S., Sidhartha, P., Saroj, P.: Optimal Gravitational Search Algorithm for Automatic Generation Control of Interconnected Power Systems, *Ain Shams Engineering Journal*, Vol. 5, No. 2, pp. 721 – 733, 2014.
- [28] Hiep, T., Thang, V., Thong, H., Tri, D.: Control of the Side Brush Street Sweeper for Various Road Surfaces Using PID and Sliding Mode Controllers”, *FME Transactions*, Vol. 51, No. 3, pp. 318-328, 2023.

NOMENCLATURE

m_u	Mass of the unsprung element	500	kg
m_s	Mass of sprung element	4500	kg
m_d	Mass of the driver	--	kg
k_u	Tire's stiffness	1600000	N/m
k_s	Vehicle suspension's stiffness	300000	N/m
k_d	The driver seat	--	N/m

	suspension's stiffness		
c_u	Tire's damping coefficient	150	Ns/m
c_s	Vehicle suspension's damping coefficient	20000	Ns/m
c_d	The driver seat suspension's damping coefficient	--	Ns/m
x_u, x_s, x_d	Displacement of the unsprung element, the sprung element, and the driver	--	m
$\dot{x}_u, \dot{x}_s, \dot{x}_d$	Velocity of the unsprung element, the sprung element, and the driver	--	m/s
$\ddot{x}_u, \ddot{x}_s, \ddot{x}_d$	Acceleration of the unsprung element, the sprung element, and the driver	--	m/s ²
$y(t)$	Road excitation	--	m
g	Gravitational acceleration	9,81	m/s ²
F	Control signal	--	N

ПРИМЕНА ГЕНЕТСКОГ АЛГОРИТМА У ВИШЕЦИЉНОЈ ОПТИМИЗАЦИЈИ СТРУКТУРНИХ ПАРАМЕТАРА И ПАРАМЕТАРА ПИД КОНТРОЛЕРА НА СИСТЕМУ ВЕШАЊА ВОЗАЧЕВОГ СЕДИШТА АУТОБУСА

Н.Д. Фам

Систем вешања возачевог седишта је оптимизован помоћу модела четвртине возила са 3 степени слободе. Циљеви оптимизације су истовремено минимизирање убрзања и померања возача. Крутост еластичног елемента k_d (N/m) и коефицијент пригушења амортизера c_d (Ns/m) су оптимизовани Парето методом са циљном функцијом $J(x)$ пројектованом методом пондерисаног квадратног збира, а минимална вредност $J(x)$ је пронађена генетским алгоритмом (GA). ПИД контролер је интегрисан у систем ради побољшања ефикасности рада, а GA оптимизује параметре контролера K_P , K_I , K_D и N . Процеси оптимизације су спроведени под условима пролазне побуде пута према стандарду IRC 99-1988. Резултати су показали да је, у поређењу са пасивним седиштем са оптимизованим структурним параметрима, активно седиште са ПИД контролером смањило вертикално померање за 80 - 88% при маси возача од 65 (кг), 100 (кг) и 72 - 84% при маси возача од 80 (кг).